2014 22nd International Conference on Pattern Recognition

Using Shape-Aware Models for Lumbar Spine Intervertebral Disc Segmentation

Rabia Haq*, David A. Besachio†, Roderick C. Borgie† and Michel A. Audette*
*Modeling, Simulation and Visualization Engineering
Old Dominion University, Norfolk, VA, USA
Email:{rhaqx001, maudette}@odu.edu
†Naval Medical Center Portsmouth, Portsmouth, VA, USA
Email: {David.Besachio, Roderick.Borgie}@med.navy.mil

***Abstract*—High incidence cases associated with back pain include intervertebral disc degeneration (IDD), or disc herniation, in the spinal lumbar region, as well as sciatica, pain in the legs due to IDD. This research aims to provide a more accurate and robust segmentation scheme for identification of spine pathologies, to assist with spine surgery planning and simulation. We are developing a minimally supervised 3D segmentation approach of lumbar spine herniated discs for MRI scans that exploits weak shape priors encoded in simplex mesh active surface models. In the event that the internal simplex shape memory influence hinders detection of pathology, user-assistance is allowed to turn off the shape feature and guide model deformation. We propose use of weak shape priors as a precursor to, and incorporation of, a shape-statistics feature for landmark-based semi-automatic segmentation of healthy intervertebral discs, and ultimately, for segmentation of vertebrae. Our framework enables the application of shape priors in the healthy part of the anatomy, and the disabling of these priors where inapplicable. Results were validated against expert-guided segmentation and demonstrate promising results with absolute mean segmentation error of less than 1 mm.**

I. Introduction

High incidence cases associated with back pain include inter-vertebral disc degeneration (IDD), or disc herniation, in the spinal lumbar region, as well as sciatica, pain in the legs due to IDD [1]. Imaging studies indicate that 40% of patients suffering from chronic back pain showed symptoms of IDD [2]. Primary treatment for lower back pain consists of non-surgical treatment methods. If non-surgical treatments are ineffective, a surgical procedure may be required to treat IDD, a procedure known as spinal discectomy. Approximately 300,000 discectomy procedures, over 90% of all spinal surgical procedures [3], are performed each year, totaling up to $11.25 billion in cost per year. Other spinal surgeries include treatment for metastatic spinal tumors and spinal cord injury.

A patient-specific, high-fidelity spine anatomical model that faithfully represents any existing spine pathology can be utilized as follows

- in surgery planning and navigation, for use by expert surgeons, and
- as an anatomical model for surgery simulation for training residents.
- To facilitate the fusion of several spine medical images into a probabilistic intensity atlas of the spine that mirrors a brain atlas [4] and that in turn could provide priors for identifying pathologies [5].

In this paper we propose a minimally supervised method for segmentation of herniated discs from high-resolution T2-weighted Magnetic Resonance Imaging (MRI). A simplex active surface mesh is initialized in the sagittal plane of a patient MRI volume, and allowed to deform using weak shape priors to capture the disc boundary. In the event that the simplex model is unable to automatically capture the boundary accurately, the user can manually guide the model deformation through constraint points placed on the image volume. We successfully demonstrate the use of weak shape priors through automatic segmentation of healthy intervertebral discs, on the basis of landmark-based registration. Our results are validated on a clinical dataset of 8 healthy disc cases and 5 herniated disc cases, and achieve mean segmentation error of less than 1 mm.

Section II introduces relevant anatomy and discusses the clinical background, section III surveys research related to intervertebral disc segmentation, section IV explains the framework of our segmentation method and section V provides research results. We discuss future work and conclusions in section VI.

II. Intervertebral disc anatomy

The initial step towards determining the cause of lower back pain is acquiring and analyzing medical image scans of the patient. The standard procedure for detecting abnormalities in the spinal structures is through visual inspection of the medical images, typically T2 weighted MRI scans, subject to the expertise of the physician. Spine treatment planning requires a patient-specific 3D anatomical model of the spine capable of correctly representing the salient anatomical features, such as the vertebrae, the inter-vertebral discs, the spinal cord and surrounding nerves. This requires identification of non-overlapping anatomical structures in medical images, a process otherwise known as *image segmentation*. Low image resolution or image noise hinder the detection of these complex structural boundaries, affecting the accuracy of the constructed model.

The intervertebral disc is a soft tissue structure between two adjacent vertebral bodies. It consists of a stronger outer layer of fibrous cartilage known as annulus fibrosus that

1051-4651/14 $31.00 © 2014 IEEE
DOI 10.1109/ICPR.2014.550

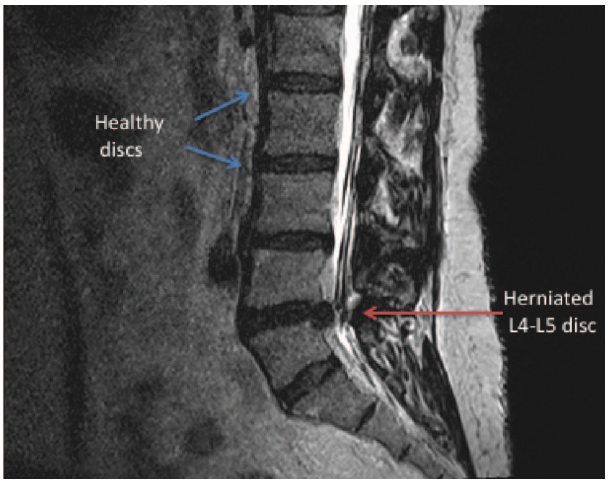

Fig. 1. Comparison of a normal and herniated lumbar disc anatomy in a T-2 weighted MRI scan. The herniated disc, located between the L4 and L5 verterae, is pinching the spinal nerve extending from the spinal cord, resulting in localized or radiating pressure and pain.

surrounds the softer, jelly-like nucleus pulposus and evenly distributes the pressure across the disc. It is the nucleus pulposus that acts as a shock-absorber between the vertebrae and ensures spinal flexibility. In this research, we consider disc herniation as a medical condition caused when the central portion of the inter-vertebral disc, nucleus pulposus, is forced out of the stronger outer fibrous ring due to pressure or a tear in the annulus fibrosus, causing the localized displacement of the disc material beyond the normal margins of the intervertebral disc space [6]. This tear in the outer ring may cause considerable pain and possible nerve root compression, resulting in localized or radiating pain in the lower back and legs. This condition usually occurs in adults as a result of a trauma or injury to the spinal column or due to wear and tear. It most often occurs in the lumbar spine as that region supports most of the weight of the spine and back, with 95% cases located at the L4-L5 disc, or the L5-S1 disc [7]. Disc herniation is commonly detected through a sagittal view of an MRI image [8]. Figure 1 depicts a sagittal T2-weighted MRI scan featuring both normal and herniated discs.

III. Related Research

3D segmentation of intervertebral discs is a prerequisite for the development of a computer-based surgery planning tool. Various inter-vertebral disc segmentation methods have been introduced, but are either limited to 2D segmentation of disc pathology, or 3D segmentation of healthy inter-vertebral discs.

Michopoulou et al. [9] proposed an atlas-based method for segmentation of degenerated lumbar intervertebral discs limited to 2D MRI scans coupled with intensity-based classifiers, with classification accuracy of 91.6% for normal and 87.2% of degenerated discs. Alomari et al. [10] proposed a herniated disc diagnostic method that classifies pathology limited to 2D MRI scans using a Bayesian classifier with a coupled active shape model and a gradient vector flow snake for segmentation.

Klinder et al. [11] and Kelm et al. [12] proposed automatic, learning-based 3D detection and segmentation frameworks of the spine, and suggested that existing disc pathologies can be reliably segmented without specifying segmentation accuracy of the pathological structure. Lalonde et al. [13] proposed kriging-based deformation of a tetrahedral template mesh of the spine, but have not demonstrated the ability to deal with pathologies such as herniated discs. Moreover, this work is based on high-resolution meshes that are essentially inapplicable to interactive surgery simulation as a result of a high element count. Neubert et al. [14] proposed a 3D automated, shape-based segmentation method for intervertebral discs and classified 7 discs as degenerated. They stated that their results indicate potential of using statistical shape-aware models for segmentation of disc pathology without explicitly addressing herniated disc segmentation accuracy. Disc pathology generally cannot be accurately represented using strong shape priors, given that there is no average disc pathology shape.

Our method demonstrates the ability to successfully segment disc pathology, based on minimally supervised, spatially variable weighting of weak prior shape information. We also exploit controlled-resolution meshing conducive to a multi-resolution approach to segmentation as well as producing anatomical models with low element count for interactive simulation.

IV. Method

Our segmentation approach is based on the discrete Simplex surface model. A Simplex deformable model can be expressed as a physically-based system, where point vertices are treated as point masses and edges model physical properties, such as a spring-like behavior, or object boundary smoothness, and is further discussed in section IV-D.

Weak shape priors in Simplex mesh deformable models are being exploited to deform an ellipsoid template mesh for segmentation of an intervertebral disc. An outline of our segmentation and validation approach is illustrated in figure 2. In the event that the simplex fails to accurately capture a herniated disc boundary, the user is allowed to manually guide the segmentation process by placing constraint points in the image volume. Similarly, ground truth for healthy intervertebral discs has also been generated by implementing this minimally-supervised technique, where the user is allowed to manually guide deformation to correct existing segmentation errors.

The remainder of this section discusses the image dataset and image preprocessing steps, followed by the automatic Simplex mesh deformation and optional user-guidance through constraint points. The data validation technique is presented to quantify the proposed framework's performance.

A. Image dataset

Our test and validation dataset consists of MR images of the lumbar spine pertaining to 5 patients with various pathologies, such as herniated discs. Herniated discs are mostly located in the L4-L5 and L5-S1 lumbar region and have been identified in the dataset under expert supervision. T2-weighted MRI scans, acquired on a 1.5T device using spin-echo scanning sequence, having a resolution of $0.5 \times 0.5 \times 0.9mm^3$

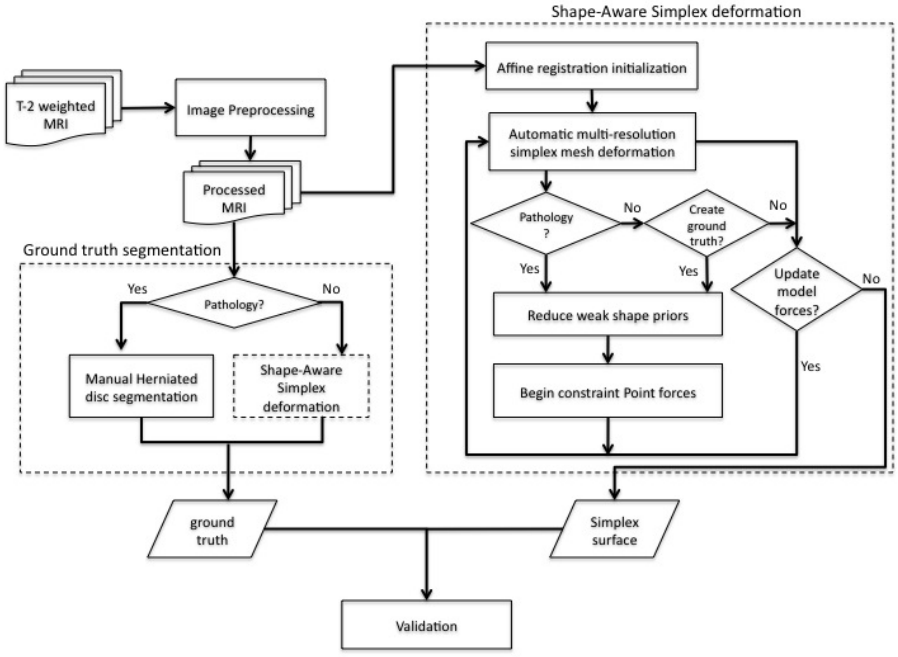

Fig. 2. Outline of our segmentation and validation approach.

have been utilized for testing and validating the segmentation approach.

A subset of 5 herniated discs and 8 healthy discs have been segmented under expert guidance [6] and supervision to be used for quantitative evaluation of the proposed minimally-supervised automatic segmentation framework, with results discussed in the section V.

B. Image preprocessing

An anisotropic diffusion [15] filter has been applied to the volumetric images to reduce image noise within the structures while preserving image boundaries. The filter mitigates image noise located around the disc by reducing the overlapping image intensities of the herniated disc boundary and the surrounding posterior ligament [8]. The Insight Segmentation and Registration Toolkit (ITK) [18] has been utilized for applying image preprocessing filters.

C. Mesh initialization through landmark-based affine registration

An ellipsoid template mesh is initialized within the herniated disc image volume for simplex mesh deformation. Arbitrary translation, rotation and scaling effects need to be captured between the template mesh and the MRI image. 6 landmarks are manually placed on the ellipsoid template mesh corresponding to 6 landmarks within the disc image boundary to initialize the template within the disc image through affine registration. These landmarks are placed at the center, superior, inferior, anterior and posterior points on the disc surface, as well as at the mostly superior disc surface to capture arbitrary rotational effects. The initialized template mesh is then allowed to automatically deform using a multi-resolution surface model, as described in section IV-D.

D. Automatic multi-resolution simplex deformation

This research exploits simplex mesh discrete deformable models for segmentation of intervertebral discs. Introduced by Delingette [16] for 3D shape reconstruction and segmentation, a k-simplex mesh is a k-manifold discrete mesh with exactly k+1 distinct neighbors. A simplex mesh has the property of constant vertex connectivity. Simplex meshes can represent various objects depending on the connectivity k, where 1-simplex represents a curve, a 2-simplex represents a surface, and a 3-simplex represents a volume. Our research is focused on surface representation for image segmentation using 2-simplex meshes with 3 constant vertex connectivity.

The constant connectivity of the 2-simplex mesh leads to three simplex parameters corresponding to a vertex with a mass and its three neighboring vertices that are invariant under similarity transformations [16]. These independent simplex parameters can be utilized to represent the geometric constraints enforced upon a vertex with respect to its three neighbor vertices. Therefore, a vertex P can be defined with respect to its neighbors P_i with its simplex parameters ϵ_1, ϵ_2 and ϕ. ϵ_i are the barycentric coordinates of the projection of vertex $P_\perp$ on the triangle $(P_1P_2P_3)$ such that $\epsilon_1 + \epsilon_2 + \epsilon_3 = 1$. ϕ is the simplex angle linked to the mean curvature at vertex P and $h = ||P_\perp - P||$ is the elevation of P and the projected vertex $P_\perp$ along the normal direction n. The shape-based constraints of P, updated by Gilles [17], are thus uniquely governed by the equation

$$P(\epsilon_1, \epsilon_2, \phi) = \epsilon_1 P_1 + \epsilon_2 P_2 + (1 - \epsilon_1 - \epsilon_2) P_3 + h(\phi) n \quad (1)$$

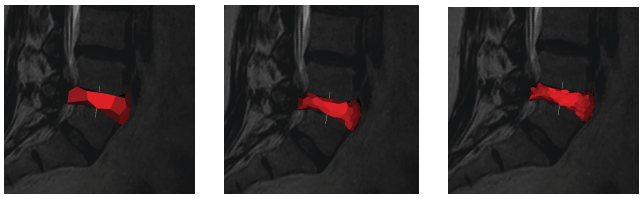

(a) (b) (c)

Fig. 3. Use of multi-resolution simplex meshes for segmentation refinement during model deformation.

The dynamics of each vertex P is governed by a Newtonian law of motion represented by the equation

$$m\frac{d^2P_i}{dt^2} = -\gamma\frac{dP_i}{dt} + \alpha\overrightarrow{F}_{int} + \beta\overrightarrow{F}_{ext} \quad (2)$$

where m is the vertex mass, γ is the damping force and α and β are the weight factors of the internal and external forces respectively. $\overrightarrow{F}_{ext}$ is the sum of external forces governed by image edge information and gradient intensity values that minimize the distance between a vertex P and maximum gradient intensity in the neighborhood of P along the normal direction. $\overrightarrow{F}_{int}$ is the sum of internal forces represented by an elastic force that enforces smoothness and weak shape-based constraints. This physically-based deformable model is governed by forces to maintain internal stabilization through $\overrightarrow{F}_{int}$. Weak shape memory is enforced by constraining the internal forces along the normal direction of vertex P. This is implemented by constraining the mean curvature at vertex P governed by the simplex angle ϕ by setting $\phi = \phi_c$, where ϕ_c is a constant [16].

Template mesh deformation is guided by the presence of MR image gradient forces estimated at each vertex in a direction along the surface normal. The global mesh resolution is adapted to the complexity of the disc shape being segmented in a coarse-to-fine segmentation approach. Thus, various simplex mesh resolutions of a disc shape have been generated through a multi-resolution scheme without loss of vertex connectivity for segmentation refinement, as demonstrated in figure 3(a), (b) and (c).

E. User-guided pathology segmentation

In the event that the internal simplex shape memory influence hinders the detection of pathology, user-assistance is allowed to turn off the shape feature and guide model deformation. Deformation is manually guided by placing *internal* and *external constraint points* on the volumetric image that gracefully constrain the deformation to correct under and over segmentation. Constraint point forces are enforced as an addition to the external force. In the current implementation, the number of constraint points applied to the images ranged between 37-60, depending on the extremity of the disc pathology that the automatic Simplex model deformation may fail to capture. While a point set of that size is still compatible with an objective of minimal supervision, we are also currently pursuing a study to establish the sensitivity to the number of constrain points, and whether a suitable choice of image force enables a reduction of this overhead. Constraint points are applied to the herniated disc image boundary to correctly guide the simplex mesh deformation, resulting in *minimally-supervised* segmentation of herniated discs using the proposed method.

Validation Metric	Healthy disc
Absolute Mean error (mm)	0.275
Absolute Std. dev. (mm)	0.418
Average Hausdorff distance (mm)	3.237

TABLE I. AVERAGE VALIDATION METRICS COMPARING SEMI-AUTOMATIC SEGMENTATION RESULTS WITH CORRESPONDING EXPERTLY-CORRECTED SEGMENTATION OF 8 HEALTHY LUMBAR INTERVERTEBRAL DISCS.

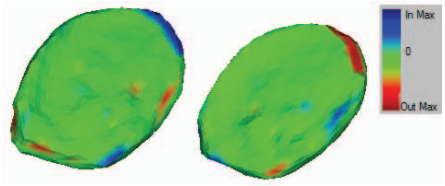

Fig. 4. Comparison of a semi-automatic L5-S1 disc segmentation result against its corresponding expertly-corrected segmentation (ground truth), with -2.452mm max. in, 2.081mm max. out error.

This minimally-supervised segmentation method has also been utilized for expert correction of healthy intervertebral disc segmentation, which serves as ground truth for validation of our healthy disc segmentation results, labeled as *expertly-corrected* segmentation. This manual correction is mostly observed at the lateral margins of the intervertebral discs as discussed in Section V.

V. RESULTS

MeshValmet [19] has been utilized for calculation of quantitative validation metrics. The absolute mean surface error (in mm) and absolute standard deviation of all errors (in mm) and the Hausdorff distance (in mm) comparison metrics have been calculated to compare the quality of our segmentation approach with ground truth. The Hausdorff distance is the maximum surface distance between two surface meshes and quantitatively represents a measure of the worst segmentation error.

Statistical comparison of 8 semi-automatic, landmark and weak shape-prior based segmentations of healthy lumbar intervertebral discs with expertly-corrected segmentation results, considered ground truth, is represented in table I. The average absolute mean error of healthy disc segmentation approach is 0.275 mm$\pm$0.418mm, with an average Hausdorff distance of 3.24 mm. The average maximum surface error was located at the lateral margins of the intervertebral disc, where the semi-automatic, unsupervised segmentation approach failed to faithfully capture the image boundary due to image intensity ambiguity caused by surrounding spine tissues and ligaments. Figure 4 compares automatic segmentation of a healthy L5-S1 disc with the expertly-corrected segmented result, considered ground truth. Our semi-automatic segmentation approach under-segmented the lateral margins with a maximum In error of -2.45 mm, and a mean segmentation error of 0.19mm$\pm$0.29mm.

Validation Metric	Herniated disc
Absolute Mean error (mm)	0.608
Absolute Std. dev. (mm)	0.518
Average Hausdorff distance (mm)	3.485

TABLE II. AVERAGE VALIDATION METRICS COMPARING MINIMALLY-SUPERVISED SEGMENTATION RESULTS WITH CORRESPONDING MANUAL SEGMENTATION OF 5 HERNIATED LUMBAR INTERVERTEBRAL DISCS.

Average results of 5 herniated discs comparing minimally-supervised segmentation results against manual segmentation have been calculated. Evaluation results have been obtained by calculating surface to mesh difference between the manual segmentation, considered ground truth, and simplex model from our approach of the corresponding intervertebral disc. Our approach demonstrates absolute mean surface error of 0.61 mm$\pm$0.52 mm of segmentation of 5 herniated intervertebral discs (Table II). Our results are favorable in comparison with competing 2D segmentation methods of herniated discs, and 3D segmentation methods of healthy discs. Michopoulou et al. [9] reported a 2D mean absolute distance of 0.61mm, whereas Neubert et al. [14] achieved a 3D segmented Hausdorff distance of 3.55mm for herniated disc segmentation.

Figure 5 demonstrates the spatial distribution of error between initial automatic segmentation using weak shape priors, minimally-supervised segmentation result after constraining model deformation, and the corresponding manual segmentation, considered ground truth, of the herniated disc results. Weak shape priors are successfully able to segment the disc with a maximum in error of -5.022mm near the disc pathology. This error is reduced to -3.369mm through minimally-supervised segmentation of pathology. It can be observed that maximum error in our minimally-supervised segmentation result is located at the lateral portion of the intervertebral disc. This is likely due to ambiguity in determining the intervertebral disc boundary at the lateral margins of the anatomy during manual segmentation. Our method also tends to overestimate the degradation of the posterior herniated disc due to internal smoothness properties, where constraint points have been introduced to correct this overestimation of the degradation of segmentation of pathology.

Robustness to variability in user supervision is demonstrated in a series of experiments where the same anatomist's results are compared over several template initializations, and where two anatomist results are also compared. Table III shows an absolute mean error of 0.265 mm between two sets of expertly-corrected segmentations performed by the same human rater. The absolute mean error between two segmentations performed by different human raters is 0.285 mm, demonstrating no significant difference between raters. As depicted in Figure 6, most intra-rater and inter-rater variability was observed at the lateral margins of the disc as well, where the user guided simplex mesh deformation in presence of ambiguous image boundary. This is consistent with the segmentation error observed in Figure 5, motivating the use of statistical shape knowledge to automatically and faithfully capture object boundary in presence of image artifacts, planned in future work.

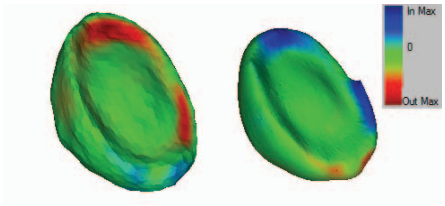

(a) Semi-automatic vs. manual segmenation

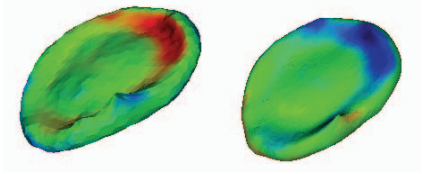

(b) Minimally-supervised vs. manual segmentation

Fig. 5. Spatial maximum out (red) and maximum in (blue) segmentation error of an L5-S1 herniated disc. (a) Comparison of semi-automatic segmentation using weak shape priors against manual segmentation (-5.022mm max. in, 2.603mm max. out). (b) Comparison of minimally-supervised segmentation against its corresponding manual segmentation (-3.369mm max. in, 3.487mm max. out).

Validation Metric	Intra-rater variability	Inter-rater variability
Absolute Mean error (mm)	0.265	0.285
Absolute Std. dev. (mm)	0.453	0.488
Maximum out error (mm)	-3.193	-3.145
Maximum in error (mm)	3.025	2.980
Hausdorff distance (mm)	3.192	3.145

TABLE III. VALIDATION METRICS COMPARING TWO SETS OF EXPERTLY-CORRECTED SEGMENTATIONS OF A HEALTHY INTERVERTEBRAL DISC PERFORMED BY THE SAME ANATOMIST AND TWO DIFFERENT ANATOMISTS, DEMONSTRATING INTER-RATER AND INTRA-RATER VARIABILITY RESPECTIVELY.

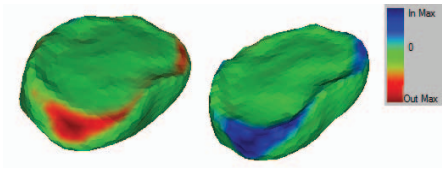

(a) Intra-rater segmentation error

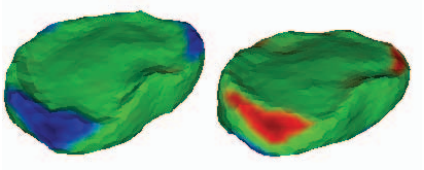

(b) Inter-rater segmentation error

Fig. 6. Maximum out (red) and maximum in (blue) segmentation error between two sets of segmentations performed by (a) the same rater (-3.192mm max. in, 3.025mm max. out), and (b) different raters (-3.145mm max. in, 2.980 max out). Over- and under-segmentation is present at the lateral margins of the healthy disc.

VI. CONCLUSION AND FUTURE WORK

In our approach, weak shape priors in active surface models are a precursor of application of statistical shape knowledge for segmentation of healthy as well as herniated discs of the lumbar spine. We believe that incorporation of statistical shape knowledge would reduce the lateral disc segmentation error,

as observed in Figures 5 and 6.

This study demonstrates use of weak shape priors in active surface models for segmentation of healthy as well as herniated discs. As herniated disc anatomy cannot be faithfully captured by prior shape or intensity features, weak shape prior influence is turned off and graceful degradation from these priors is allowed in a user-controlled manner, refining the segmentation result. Our main contribution is a framework for 3D segmentation of herniated discs of the lumbar spine, towards creating a 3D segmentation framework for development of a patient-specific surgery simulator that captures spine pathology with fidelity.

REFERENCES

[1] Luoma, K., Riihimäki, H., Luukkonen, R., Raininko, R., Viikari-Juntura, E., and Lamminen, A.: Low back pain in relation to lumbar disc degeneration. Spine, 25(4):487–492 (2000)

[2] Freemont, A. J., Watkins, A., Le Maitre, C., Jeziorska, M., and Hoyland, J. A.:Current understanding of cellular and molecular events in intervertebral disc degeneration: implications for therapy. J Pathol., 196(4):374–379 (2002)

[3] An, H., and Anderson, P.: Disc degeneration. Spine, 2677–2678 (2004)

[4] Evans, A. C., Collins, D. L., Mills, S. R., Brown, E. D., Kelly, R. L., and Peters, T. M.: 3D statistical neuroanatomical models from 305 MRI volumes. In: Proceedings of the IEEE Nucleur Science Symposium and Medical Imaging Conference, pp.1813–1817 (1993)

[5] Prastawa, M., Bulliet,E., Ho, S., Gerig, G.: A brain tumor segmentation framework based on outlier detection. Medical Image Analysis, 8(3):275–283 (2004)

[6] Fardon, D. F., and Milette, P. C.: Nomenclature and Classification of Lumbar Disc pathology. Spine 26(5) pp E93–E113 (2001)

[7] Moore, K. L., and Agur, A. M. R.: Essential clinical anatomy. Lipp. Will. and Wilkins, 3rd. edition (2007)

[8] Niadich, T. P., Castillo, M., Cha, S., Raybaud, C., Smiriniotopoulos, J. G., Kollias, S. and Kleinman, G. M.: Imaging of the Spine. Elsevier (2010)

[9] Michopoulou, S.K., Costaridou, L., Panagiotopoulos, E., Speller, R., Panayiotakis, G., and Todd-pokropek, A. In: IEEE transactions on Biomedical Engineering, 56(9), pp 2225-2231 (2009)

[10] Alomari, R. S., Corso, J. J., Chaudhary, V., and Dhillon, G.: Lumbar Spine Disc Herniation Diagnosis with a joint Shape Model. In: Proceedings of Medical Image Computing and Computer Aided Intervention Workshop on Computational Spine Imaging, (2013)

[11] Klinder, T., Ostermann, J., Ehm, M., Franz, A., and Kneser, R.: Automated model-based vertebra detection, identification, and segmentation in CT images. Medical Image Analysis, 13, pp 471–482, 2009

[12] Kelm, M. B., Wels, M., Zhou, S. K., Seifert, S., Suehling, M., Zheng, Y.: Spine detection in CT and MR using iterated marginal space learning. Medical Imaging Analysis, 17(8) pp 1283–92 (2013)

[13] Lalonde,N. M., Petit, Y., Aubin, C., Wagnac, E., and Arnoux, P. J.: Method to Geometrically Personalize a Detailed Finite-Element Model of the Spine. In: IEEE Trans. Biomed. Engineering, 60(7), pp: 2014–2021 (2013)

[14] Neubert, A., Fripp, J., Shen, K., Salvado, O., Schwarz, R., Lauer, L., Engstrom, C., and Crozier, S.: Automated 3D Segmentation of Vertebral Bodies and Intervertebral Discs from MRI. In: Digital Image Computing Techniques and Applications (DICTA), 2011 International Conference,19-24 (2011)

[15] Perona, P., and Malik, J.:Scale-space and edge detection using anisotropic diffusion. In: IEEE Transactions on Pattern Analysis and Machine Intelligence, 12(7), pp: 629–639 (1990)

[16] Delingette, H.: General object reconstruction baded on simplex meshes. International Journal of Computer Vision, 32(2), pp: 111–146 (1999)

[17] Gilles, B., and Magnenat-Thalmann, N.: Muskuloskeletal MRI segmentation using multi-resolution simplex meshes with medial representations. Med- ical Image Analysis, 14(3) pp: 291–302 (2010)

[18] Insight Segmentation and Registration Toolkit, www.itk.org

[19] MeshVelmet: Validaton Metric for Meshes, http://www.nitrc.org/projects/meshvalmet/